THE JOURNAL OF PHYSICAL CHEMISTRY A

Article

Cite This: J. Phys. Chem. A 2018, 122, 1813−1820

pubs.acs.org/JPCA

Nature of Intramolecular Resonance Assisted Hydrogen Bonding in Malonaldehyde and Its Saturated Analogue

Published as part of The Journal of Physical Chemistry virtual special issue "Manuel Yáñez and Otilia Mó Festschrift".

Alice A. Grosch,[†] Stephanie C. C. van der Lubbe,*[,†] and Célia Fonseca Guerra*[,†,‡]

[†]Department of Theoretical Chemistry and Amsterdam Center for Multiscale Modeling, Vrije Universiteit Amsterdam, 1081 HV Amsterdam, The Netherlands

[‡]Leiden Institute of Chemistry, Gorlaeus Laboratories, Leiden University, 2333 CC Leiden, The Netherlands

Supporting Information

ABSTRACT: The nature of resonance-assisted hydrogen bonds (RAHB) is still subject of an ongoing debate. We therefore analyzed the σ and π charge redistributions associated with the formation of intramolecular hydrogen bonds in malonaldehyde (MA) and its saturated analogue 3-hydroxypropanal (3-OH) and addressed the question whether there is a resonance assistance phenomenon in the sense of a synergistic interplay between the σ and π electron systems. Our quantum chemical calculations at the BP86/TZ2P level of theory show that the π charge flow is indeed in line with the Lewis structure as proposed by the RAHB model. This typical rearrangement of charge is only present in the unsaturated system, and not in its saturated analogue. Resonance in the π electron system assists the intramolecular hydrogen bond by reducing the hydrogen bond distance, and by providing an additional stabilizing component to the net bonding energy. The σ orbital interaction plays an important role in the enhanced hydrogen bond strength in MA as well. However, there is no resonance assistance in the sense of an interplay between σ charge transfer and π polarization; σ and π contribute independently from each other.

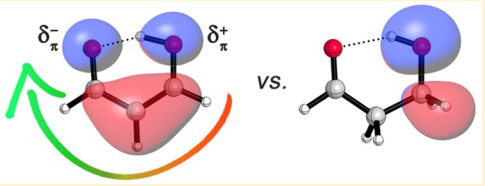

I. INTRODUCTION

Hydrogen bonds play a crucial role in biochemical processes[1−3] and many applicative fields in supramolecular chemistry.[4−10] A thorough understanding of the hydrogen bonding mechanism is therefore essential.

Hydrogen bonds are generally described as electrostatic interactions with partly covalent character.[11,12] The electrostatic interactions occur between the partially positively charged hydrogen atom HA and the opposing partially negatively charged hydrogen acceptor atom A, where A is an electronegative atom such as N or O. The charge-transfer interactions, which have been shown to be important by experimental and theoretical studies, take place between the σ lone pair orbital on A and the antibonding σ^* orbital on the opposing HA bond (Figure 1a).[11−17] Other components have been shown to influence the hydrogen bond strength as well, including dispersion interactions[18] and Pauli (steric) repulsion[19] (Figure 1b).

Another factor that is believed to be important is resonance assistance by the π electrons. This so-called resonance assisted hydrogen bonding (RAHB) model, as first proposed by Gilli et al.,[20,21] states that "*the interplay between hydrogen bond and (...) heteroconjugated systems can strengthen remarkably the hydrogen bond itself.*" In other words, the model suggests that there is a synergistic reinforcement between hydrogen bonding and π delocalization.

However, the nature of the π assistance has been the subject of an ongoing debate.[22−29] One interpretation of RAHB is that the delocalization of the π system assists the hydrogen bond by making the proton acceptor more negative and the proton donor more positive, which results in a stronger electrostatic interaction, and thus a shortening of the hydrogen bond distance, and thus an overall increase in hydrogen bond strength.[20,21,24−26] For malonaldehyde (MA), which is the simplest representative of RAHB and subject of our study, this form of resonance assistance is shown in Figure 1c.

Another interpretation of RAHB is that there is a synergistic interplay between the donor−acceptor interactions in the σ and polarization in the π electron system. In this exposition, π resonance assists the hydrogen bond by pushing the proton acceptor's lone pair orbital σ_{LP} up in energy, which results in a smaller HOMO−LUMO gap and thus a stronger σ charge-transfer interaction.[20] For intermolecular hydrogen bonds in Watson−Crick base pairs, this so-called cooperative reinforcement has been shown to be very small, even though the buildup of charge in the σ electron system is indeed counteracted and compensated by polarization in the π electron system.[14,27]

In this study, we have investigated the σ and π charge redistributions associated with the formation of intramolecular

Received: December 22, 2017
Revised: January 22, 2018
Published: January 22, 2018

DOI: 10.1021/acs.jpca.7b12635
J. Phys. Chem. A 2018, 122, 1813−1820

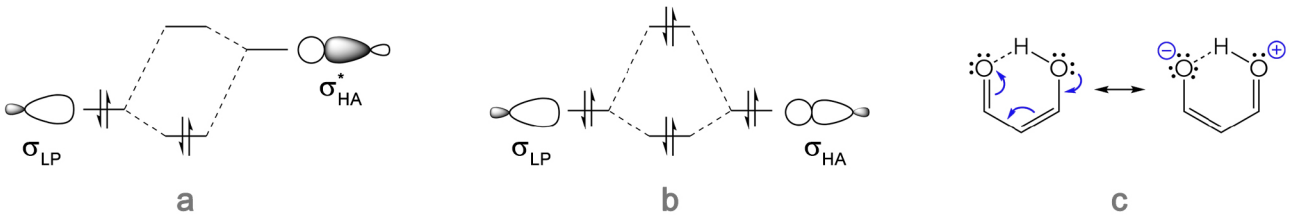

Figure 1. Schematic overview of (a) donor−acceptor interactions, (b) steric interactions, and (c) resonance assistance by π polarization in hydrogen-bonded systems.

hydrogen bonds and addressed the question whether there is a resonance assistance phenomenon in the sense of a synergistic interplay between the σ and π electron systems. We have studied two systems, namely, MA and 3-hydroxypropanal (3-OH), which is the saturated analogue of MA (Figure 2). On the basis of the downfield ^{1}H NMR chemical shift, decrease of OH vibrational frequency, and geometrical characteristics, the intramolecular hydrogen bond in MA is generally considered to be stronger than its saturated counterpart.[20,25,28,29] Our computations are in line with these findings, because the optimized MA has longer O−H and shorter O···H and O,O bonds than 3-OH (Figure 2).

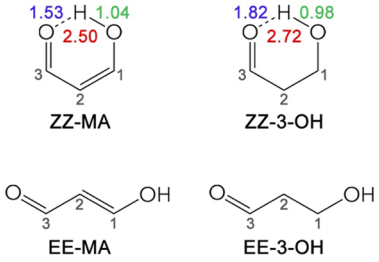

Figure 2. Hydrogen bond (O, O) distances in red, OH distances in green, and O···H distances in blue [Å] for malonaldehyde (MA) and 3-hydroxypropanal (3-OH) in *ZZ* and *EE* conformation at the BP86/TZ2P level of theory. The *EE* conformations are obtained by rotating the *ZZ* conformations 180° around the C_1-C_2 and C_2-C_3 bond axes.

Here, we demonstrate that the enhanced hydrogen bond strength in MA is indeed partly caused by π resonance assistance, which makes the hydrogen bond shorter and provides an additional stabilizing component to the total bonding energy. This is in line with the recent work by Jiang and co-workers.[25,26] The intramolecular hydrogen bond in MA is further enhanced by σ orbital interactions. There is, however, no resonance assistance in the sense of a synergistic interplay between the σ and π electronic systems; the σ and π interactions enhance the intramolecular hydrogen bond in MA independently from each other.

II. COMPUTATIONAL METHODS

IIa. Computational Settings. All calculations were performed with the density functional theory (DFT) based program Amsterdam density functional (ADF) 2016.101.[30] We used the BP86 generalized gradient approximation (GGA) density functional, which is composed of the Becke[31] (B) exchange and Perdew[32] (P86) correlation functional. The BP86 functional is in good agreement with the best available ab initio results for hydrogen bond lengths and energies of DNA base pairs.[33−35]

The Kohn−Sham molecular orbitals (KS MOs) were constructed from a linear combination of Slater-type orbitals (STOs), which have the correct cusp behavior and long-range decay. We used the TZ2P basis set, which is of triple-ζ quality for all atoms and has been augmented with two sets of polarization functions, i.e., 2p and 3d on H and 3d and 4f on C and O.[36] To speed up the computation, we treated the 1s core−shells of C and N by the frozen-core approximation.[37]

Geometries were optimized in gas phase in delocalized coordinates. The convergence criterion was 1×10^{-5} for the nuclear gradient in hartrees/ångströms. We optimized the systems in C_s symmetry, because the C_s symmetry allows us to decompose the orbital interaction into a σ and π contribution (*vide infra*). For 3-OH, the C_s symmetry is not a global minimum structure; the energetic penalty for enforcing a planar geometry is 5.7 kcal mol^{-1}. However, as we are only interested in the nature of the intramolecular hydrogen bond and how it compares with its unsaturated analogue MA, we enforced a planar structure with C_s symmetry for all structures in this work. The molecular figures were illustrated using CYLview.[38] Full computational details are available in the Supporting Information.

IIb. Energy Decomposition Analysis (EDA). To study the origin of the stronger hydrogen bond in MA, we examined the bond energy of each system in the framework of Kohn−Sham molecular orbital theory using the quantitative energy decomposition analysis (EDA) scheme.[39] In this fragment-based approach, the interaction energy ΔE_{int} is decomposed into three physically meaningful and chemically intuitive terms, namely, the electrostatic interaction ΔV_{elstat}, Pauli repulsion ΔE_{Pauli}, and orbital interactions ΔE_{oi}:

$$\Delta E_{int} = \Delta V_{elstat} + \Delta E_{pauli} + \Delta E_{oi} \quad (1)$$

The term ΔV_{elstat} corresponds to the classical electrostatic interactions between the fragments' unperturbed charge distributions and is usually attractive. The Pauli repulsion ΔE_{Pauli} comprises the destabilizing interactions between overlapping, occupied orbitals, and is responsible for any steric repulsion. The orbital interaction ΔE_{oi} accounts for charge transfer (i.e., donor−acceptor interactions between occupied orbitals on one fragment and unoccupied orbitals on the other fragment) and polarization (empty-occupied orbital mixing on one fragment due to the presence of the other fragment). A theoretical overview of this energy decomposition is given in the Supporting Information and in ref 39.

The orbital interaction energy can be further decomposed into the contributions from each irreducible representation Γ of the point group of the corresponding system. For planar systems with C_s symmetry, this effectively means that we can decompose ΔE_{oi} into a σ and π contribution:

$$\Delta E_{oi} = \Delta E_{\sigma} + \Delta E_{\pi} \quad (2)$$

DOI: 10.1021/acs.jpca.7b12635
J. Phys. Chem. A 2018, 122, 1813−1820

Because the hydrogen bond is intramolecular, it is not possible to define the fragments such that they interact through the hydrogen bond only. Instead, the fragments are obtained by breaking the C_2-C_3 bond (Figure 2 for atomic numbering), resulting in two radical fragments (Figure 3). In this approach, the recombination of the fragments involves not only the formation of the hydrogen bond but also the C_2-C_3 bond.

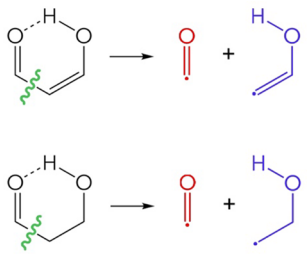

Figure 3. Radical fragments are obtained by breaking the C_2-C_3 bond in MA and 3-OH (green lines), resulting in ketone fragments (red) and enol fragments (blue).

IIc. Removing π Virtual Orbitals. Cooperative effects between the σ and π electron systems were studied by switching off (i.e., deleting) the virtual π orbitals. This approach inhibits any delocalization of charge in the π electron system and thus removes the possibility of resonance assistance by π polarization. The synergistic interplay ΔE_{syn} between σ and π is then defined as

$$\Delta E_{syn} = \Delta E_{\sigma}(\sigma,\pi;\sigma,\pi) - (\Delta E_{\sigma}(\sigma,-;\sigma,-)) \quad (3)$$

where $\Delta E_{\sigma}(\sigma,\pi;\sigma,\pi)$ is the σ orbital interaction energy when all virtual orbitals are present, and $\Delta E_{\sigma}(\sigma,-;\sigma,-)$ is the σ orbital interaction energy when all π virtual orbitals are removed. A negative ΔE_{syn} corresponds to a stabilizing cooperative effect, and thus to resonance assistance in the sense of interplay between the σ and π electron systems.

At this point, it is useful to note that the computation of the individual energy terms in eq 1 occurs stepwise, where first the electrostatic interaction ΔV_{elstat}, then the Pauli repulsion ΔE_{Pauli} and last, the orbital interactions ΔE_{oi} are computed (see also Supporting Information). This means that ΔV_{elstat} and ΔE_{Pauli} remain by definition unchanged upon removal of the π virtual orbitals. Therefore, we have only studied the effect of resonance assistance by π polarization on the σ charge-transfer interactions, i.e., the synergistic interplay between σ and π.

IId. Voronoi Deformation Density (VDD) Charges. The atomic charge distribution was analyzed by using the Voronoi deformation density (VDD) method.[40] The VDD method partitions the space into so-called Voronoi cells, which are nonoverlapping regions of space that are closer to nucleus A than to any other nucleus.[41] The charge distribution is determined by taking a fictitious promolecule as reference point, in which the electron density is simply the superposition of the atomic densities. The change in density in the Voronoi cell when going from this promolecule to the final molecular density of the interacting system is associated with the VDD atomic charge Q. Thus, the VDD atomic charge Q_A^{VDD} of atom A is given by

$$Q_A^{VDD} = -\int_{\text{Voronoi cell of A}} [\rho(r) - \rho_{promolecule}(r)]\, dr \quad (4)$$

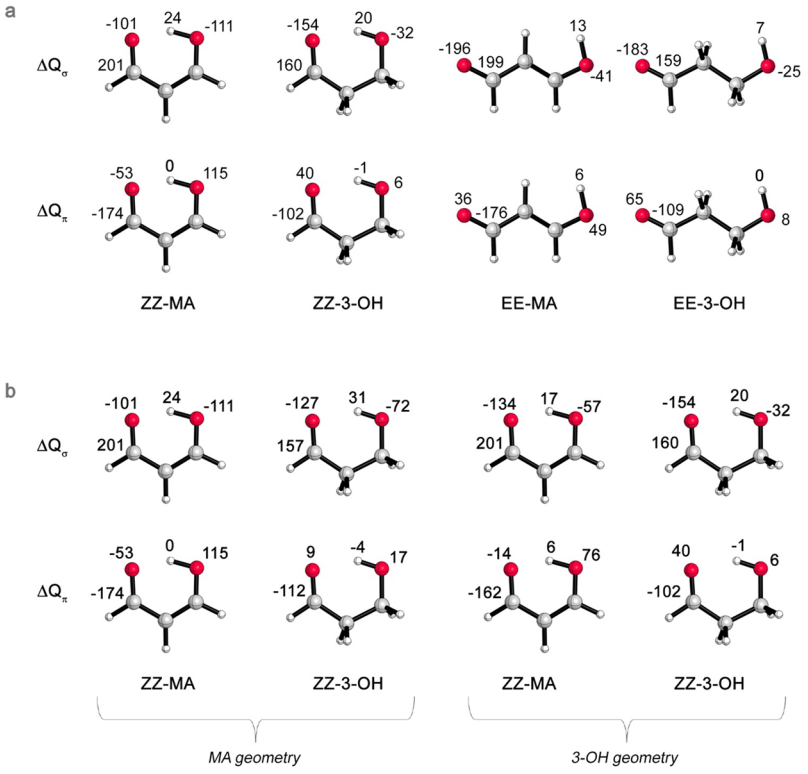

Figure 4. Voronoi deformation density (VDD) atomic charges ΔQ [milli-au] associated with the formation of the molecules from their radical fragments at the BP86/TZ2P level of theory. (a) MA and 3-OH in closed (*ZZ*) and open (*EE*) conformation with optimum hydrogen bond lengths. The *EE* conformations are obtained by rotating the *ZZ* conformations 180° around the C_1-C_2 and C_2-C_3 bond axes. (b) MA and 3-OH frozen in MA distance (left) and 3-OH distance (right). Only the hydrogen atoms at C_1 and C_2 have been reoptimized for the frozen geometries.

DOI: 10.1021/acs.jpca.7b12635
J. Phys. Chem. A 2018, 122, 1813−1820

So, instead of computing the amount of charge contained in an atomic volume, we compute the flow of charge from one atom to the other upon formation of the molecule. The physical interpretation is therefore straightforward. A positive atomic charge Q_A corresponds to the loss of electrons, whereas a negative atomic charge Q_A is associated with the gain of electrons in the Voronoi cell of atom A.

The VDD scheme can be extended to the analysis of bonding between molecular fragments by computing the change in electron density that is associated with the formation of the bond. In this approach, we take the sum of the prepared fragments are initial density ρ_i:

$$\Delta Q_A^{VDD} = -\int_{\text{Voronoi cell of A in complex}} \left[\rho_{complex}(r) - \sum_{\text{fragments}} \rho_i(r) \right] dr \quad (5)$$

which offers a direct insight into the redistribution of electronic density caused by the bond formation between the fragments. As a further analysis tool, the ΔQ_A^{VDD} of atom A can be decomposed into contributions of different irreducible representations Γ of the point group of the complex. For planar molecules, this affords a distinction to be made between σ and π components.

III. RESULTS AND DISCUSSION

IIIa. Charge Redistribution. We have analyzed the redistribution of the σ and π electron density in MA and its saturated analogue 3-OH by using the VDD method (section IId). The VDD charges, as shown in Figure 4, represent the change in density upon formation of the fully interacting system from the radical fragments as defined in Figure 3 (see also eq 5). Because our fragment-based approach measures not only the hydrogen bond but also the formation of the C_2-C_3 bond, we also analyzed MA and 3-OH in open (*EE*) conformation by rotating the closed (*ZZ*) conformers 180° around the C_1-C_2 and C_2-C_3 bonds. This approach cancels out the intramolecular hydrogen bond and thus allows us to study the effect of the intramolecular hydrogen bond on the flow of density in the σ and π electron systems.

For MA, there is a larger σ charge flow ΔQ_σ to the carbonyl's oxygen atom =O in open (196 milli-au) than in closed (101 milli-au) conformation (Figure 4a). This is in line with the σ charge-transfer interaction as shown in Figure 1a, in which the lone pair orbital donates charge to the opposing empty σ^* orbital on OH. For 3-OH, the σ charge flow ΔQ_σ to the carbonyl's oxygen atom is also larger in open (183 milli-au) than in closed (154 milli-au) conformation, but the difference is smaller than observed for MA. This means that the net transfer of charge is larger in the intramolecular hydrogen bond in MA than in 3-OH.

Next, we analyze the transfer of charge in the π electron system, ΔQ_π. As can be seen in Figure 4a, the carbonyl's oxygen atom in *ZZ*-MA becomes more negatively charged (−53 milli-au), while the enol's oxygen atom becomes more positively charged (115 milli-au). This π charge rearrangement is in agreement with the Lewis structure as proposed in the RAHB model (Figure 1c).

Interestingly, this typical rearrangement of π charge disappears when intramolecular hydrogen bonding is inhibited; the carbonyl's oxygen atom in *EE*-MA becomes now positively, instead of negatively charged. The same effect is observed in the saturated systems 3-OH, i.e., both oxygen atoms in *ZZ*-3-OH and *EE*-3-OH become partially positively charged. The charge rearrangement in the π electron system in *EE*-MA and both 3-OH conformations is thus such that it counteracts the buildup of charge in the σ electron system. This has been observed before in intermolecular hydrogen-bonded systems.[27,40]

Because MA has shorter hydrogen bond lengths than 3-OH (Figure 2), we investigated whether the trends in charge redistributions remain the same when both systems share the same bond lengths. This was done by freezing *ZZ*-MA and *ZZ*-3-OH in each other's equilibrium geometry, in which we only reoptimized the hydrogen atoms on C_2 and C_3. As can be seen in Figure 4b, the charge rearrangements are more pronounced when MA and 3-OH are frozen in the MA geometry, i.e., the geometry with shorter hydrogen bond lengths. This is caused by the distance dependence of the orbital overlap, which increases when the bond length is decreased. However, the trends as observed at equilibrium bond lengths remain unchanged.

The σ charge flow ΔQ_σ to the carbonyl's oxygen atom =O is again larger in 3-OH than in MA when both systems share the same bond lengths. So, the net transfer of charge is effectively larger in the intramolecular H-bond of MA than in its saturated analogue. To understand the origin of the stronger charge-transfer interaction in MA, we studied the energies of and overlap between the lone pair orbital σ_{LP} on the carbonyl (HOMO) and antibonding orbital σ^*_{OH} (LUMO) on the opposing OH group.

As can be seen in Figure 5a, the LUMO of MA is 0.3 eV lower in energy than the LUMO of 3-OH, which results in a smaller HOMO−LUMO gap. In addition, the LUMO on MA is more diffuse than the LUMO on 3-OH, which allows for a better overlap with the opposing lone pair orbital. This

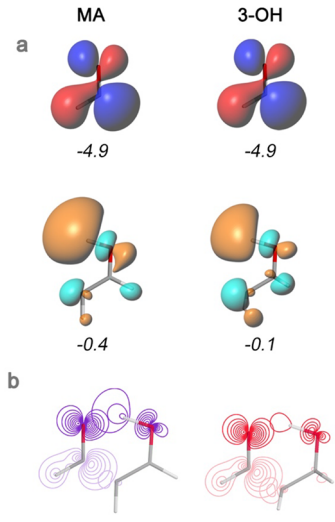

Figure 5. Characteristics of the carbonyl's lone pair orbital σ_{LP} (HOMO) and opposing OH antibonding orbital σ^*_{OH} (LUMO) of MA (up) and 3-OH (down) frozen in MA geometry at the BP86/TZ2P level of theory. (a) Isosurfaces [at 0.04 au] and energies in italic [eV] of HOMO and LUMO orbitals of the prepared fragments. (b) Contour plots [20 contours from 0.09 to 1.0 au] of the overlapping HOMO and LUMO orbitals.

DOI: 10.1021/acs.jpca.7b12635
J. Phys. Chem. A 2018, 122, 1813−1820

Table 1. Bond energy Decomposition Analysis [kcal mol^{-1}] for MA and 3-OH in *ZZ* (Closed) and *EE* (Open) Conformation with All Virtual Orbitals Present [(σ, π)] and with All π Virtual Orbitals Removed [(σ, −)] at the BP86/TZ2P Level of Theory

	ZZ-MA (closed)		*ZZ*-3-OH (closed)		*EE*-MA (open)		*EE*-3-OH (open)	
	(σ, π)	(σ, −)	(σ, π)	(σ, −)	(σ, π)	(σ, −)	(σ, π)	(σ, −)
ΔE_{int}	−128.9	−93.3	−97.1	−83.8	−116.7	−88.8	−93.2	−81.2
ΔV_{elstat}	−217.6	−217.6	−179.2	−179.2	−197.4	−197.4	−170.1	−170.1
ΔE_{Pauli}	388.3	388.3	318.3	318.3	345.1	345.1	304.1	304.1
ΔE_{σ}	−262.3	−264.0	−221.9	−222.8	−233.7	−236.5	−214.3	−215.1
ΔE_{π}	−37.3		−14.3		−30.8		−12.9	

Table 2. Bond Energy Decomposition Analysis [kcal mol^{-1}] for MA and 3-OH in *ZZ* (Closed) and *EE* (Open) Conformation Frozen in MA Geometry and 3-OH Geometry with All Virtual Orbital Present [(σ, π)] and with All π Virtual Orbitals Removed [(σ, −)] at the BP86/TZ2P Level of Theory

	ZZ-MA (closed)		*ZZ*-3-OH (closed)		*EE*-MA (open)		*EE*-3-OH (open)	
	(σ, π)	(σ, −)	(σ, π)	(σ, −)	(σ, π)	(σ, −)	(σ, π)	(σ, −)
				MA Distance (Short H-Bond)				
ΔE_{int}	−128.9	−93.3	−95.5	−75.7	−116.7	−88.8	−93.4	−77.7
ΔE_{σ}	−262.3	−264.0	−267.6	−269.3	−233.7	−236.5	−241.6	−243.5
ΔE_{π}	−37.3		−21.6		−30.8		−17.6	
				3-OH Distance (Long H-Bond)				
ΔE_{int}	−123.0	−96.7	−97.1	−83.8	−115.0	−92.0	−93.2	−81.2
ΔE_{σ}	−217.2	−218.6	−221.9	−222.8	−209.3	−210.7	−214.3	−215.1
ΔE_{π}	−27.6		−14.3		−24.5		−12.9	

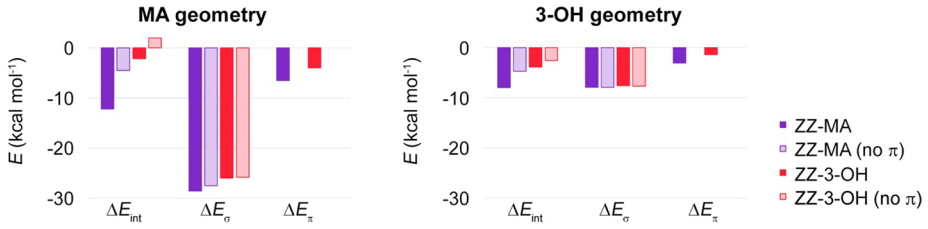

Figure 6. Hydrogen bond energies for MA (purple) and 3-OH (red) with π polarization allowed (solid fill) and disabled (pattern fill) with the systems frozen in MA geometry (left) and 3-OH geometry (right) at the BP86/TZ2P level of theory. Hydrogen bond energies are estimated by taking the difference between the *ZZ* and *EE* conformations.

becomes evident in Figure 5b, which depicts the contour plots of the overlapping orbitals when both systems are frozen in MA geometry (the contour plots of MA and 3-OH frozen in 3-OH geometry are given in the Supporting Information). Both factors, i.e., the smaller HOMO−LUMO gap and better orbital overlap, contribute to a more favorable charge-transfer interaction in MA.

The charge transfer in the π electron system ΔQ_{π} is again in agreement with the RAHB model. For MA, the π resonance makes the carbonyl's oxygen atom more negative, and the enol's oxygen more positive. However, both oxygen atoms in the saturated 3-OH become more positive. The difference in π charge flow between MA and 3-OH is smaller when both systems share identical bond lengths but is still pronounced.

On the basis of these findings, we can conclude that there is indeed resonance assistance by the π electron system in MA by making the hydrogen bond donor atom more positive, and hydrogen bond acceptor atom more negative. In the next section, we investigate whether this π resonance enforces the hydrogen bond by enhancing the σ orbital interactions. In other words, we address the question whether there is resonance assistance in the sense of a synergistic interplay between the σ and π electron systems.

IIIb. Synergistic Interplay between σ and π Electron Systems. To address the question whether there is a resonance assistance phenomenon in the sense of a synergistic interplay between the σ and π electron systems, we employed the energy decomposition analysis on the optimized structures in both closed (*ZZ*) and open (*EE*) conformation. Recall that the *EE* conformations are obtained by rotating the *ZZ* conformers 180° around the C_1−C_2 and C_2−C_3 bonds. Because this approach cancels out the intramolecular hydrogen bond, the hydrogen bond energy can be estimated by computing the energy difference between the *ZZ* and *EE* conformers. We have also used a second approach, in which the intramolecular hydrogen bond is canceled out by substituting the OH group by a H atom. This approach leads to the same trends as our comparison between *ZZ* and *EE*; the data set is given in the Supporting Information.

As can be seen in Table 1, the estimated intramolecular hydrogen bond energy (*ZZ* minus *EE*, *vide supra*) is −12.2 kcal mol^{-1} for MA and −3.9 kcal mol^{-1} for 3-OH. So, the hydrogen bond energy is stronger for the unsaturated system, which is in line with the RAHB model and stronger σ charge-transfer interaction (section IIIa).

To determine whether this stronger ΔE_{int} is caused by a cooperative reinforcement between the σ and π electron systems, we switched off all π virtual orbitals. Interestingly, the σ orbital interactions are not weakened when resonance assistance by the π electron system is inhibited (Table 1). In

DOI: 10.1021/acs.jpca.7b12635
J. Phys. Chem. A 2018, 122, 1813−1820

fact, ΔE_σ becomes more stable by 1.7, 0.9, 2.8, and 0.8 kcal mol^{-1} for *ZZ*-MA, *ZZ*-3-OH, *EE*-MA, and *EE*-3-OH, respectively. This means that the σ orbital interactions do not gain additional stabilization from the π polarization.

Comparing MA in closed (*ZZ*) and open (*EE*) conformation, we see that its increase in orbital interaction upon removal of the π virtual orbitals is 1.1 kcal mol^{-1} weaker in *ZZ* than in *EE* conformation. In comparison with the absolute σ orbital interaction energies and differences in interaction strengths, this number is negligibly small. So, the σ orbital interactions in the hydrogen bond are not reinforced by polarization in the π electron system, and in this sense, there is thus no synergistic resonance assistance.

Because MA has shorter hydrogen bond distances than 3-OH (Figure 2), and the energy terms are distance dependent, we redid the bonding analyses on MA and 3-OH while frozen in each other's equilibrium geometry. In this approach, we only reoptimized the hydrogen atoms on C_2 and C_3 (see also section IIIa), which allows us to compare MA and 3-OH with identical bond lengths. The full data set is given in the Supporting Information; the most important results are given in Table 2 and Figure 6.

As can be seen in Figure 6 and Table 2, the estimated hydrogen bond interaction energies (*ZZ* minus *EE*, *vide supra*) are −12.2 and −2.1 kcal mol^{-1} for MA and 3-OH in MA geometry, and −8.0 and −3.9 kcal mol^{-1} for MA and 3-OH in 3-OH geometry. So, the hydrogen bond in MA is ca. 10 kcal mol^{-1} (MA geometry) and 4 kcal mol^{-1} (3-OH geometry) stronger than in its saturated counterpart when both systems share the same hydrogen bond lengths. The enhanced interaction strength of MA is for an important part caused by the polarization in the π electron system ΔE_π, which is significantly stronger for MA than for 3-OH.

However, when the π virtual orbitals are switched off, the hydrogen bond strength is still stronger for MA than for 3-OH by ca. 7 (MA geometry) and 2 (3-OH geometry) kcal mol^{-1}. This means that there are also other factors that enhance the intramolecular hydrogen bond strength of MA. One of these factors is the σ orbital interaction ΔE_σ, which is stronger in MA due to a lower energy gap and better overlap between the HOMO and LUMO (section IIIa). Because ΔE_σ remains stronger for MA when the π virtual orbitals are switched off (Figure 6), we conclude again that there is no synergetic interplay between the σ and π electron systems. The remaining part of the enhanced interaction energy ΔE_{int} must come from the electrostatic interaction ΔV_{elstat} and/or Pauli repulsion ΔE_{Pauli}. These terms are influenced by differences in geometry, including the additional hydrogen atoms in the saturated 3-OH.

Nevertheless, we emphasize that, next to the σ skeleton,[28,29,42−46] the resonance in the π electron system does play a significant role in the enhanced stability of MA. This becomes even more evident when MAs in equilibrium geometry (short bond lengths) and frozen geometry (long bond lengths) are compared. The equilibrium position is favored by 5.9 kcal mol^{-1} when polarization in the π electron system is allowed. However, when π polarization is inhibited by switching off the π virtual orbitals, the 3-OH geometry becomes more favorable by 3.4 kcal mol^{-1}. This shows that π resonance does reduce the bonding distance and thus plays an important role in the enhanced interaction strength of the unsaturated system MA. These findings are in line with Jiang and co-workers.[25,26]

IV. SUMMARY AND CONCLUSIONS

We have investigated the nature of π resonance assistance in the intramolecular hydrogen bond in MA and its saturated analogue 3-OH. Our quantum chemical computations at the BP86/TZ2P level of theory show that the π charge flow is in line with the Lewis structure as proposed by the RAHB model; i.e., the proton donor OH becomes more positively charged, and the proton acceptor =O becomes more negatively charged. This typical rearrangement of charge is only present in the unsaturated system, and not in its saturated analogue.

Resonance in the π electron system assists the intramolecular hydrogen bond by reducing the hydrogen bond distance and by providing an additional stabilizing component to the net bonding energy. However, there are also other factors that play a role in the enhanced hydrogen bond strength for MA. One of these factors is the σ orbital interaction, which is stronger for MA than for 3-OH due to (1) a smaller HOMO−LUMO gap and (2) a better overlap due to the more diffuse nature of the LUMO of MA.

When π polarization is inhibited by removing all π virtual orbitals, no significant changes are observed in the σ orbital interactions. We therefore conclude that there is no synergistic interplay between the charge transfer in the σ, and polarization in the π electron system. Instead, the π polarization and σ charge-transfer interactions enhance the intramolecular hydrogen bond in MA independently from each other.

■ ASSOCIATED CONTENT

Supporting Information

The Supporting Information is available free of charge on the ACS Publications website at DOI: 10.1021/acs.jpca.7b12635.

Full computational details, theoretical overview EDA scheme, contour plots of MA and 3-OH frozen in 3-OH geometry, data set $MA_{minusOH}$ and $3\text{-}OH_{minusOH}$, data set MA and 3-OH while frozen in each other's equilibrium, and Cartesian coordinates of all systems used in this work (PDF)

■ AUTHOR INFORMATION

Corresponding Authors

*S. C. C. van der Lubbe. E-mail:s.c.c.vander.lubbe@vu.nl. Phone: 0031-20-5987627.

*C. Fonseca Guerra. E-mail:c.fonsecaguerra@vu.nl. Phone: 0031-20-5987627.

ORCID

Célia Fonseca Guerra: 0000-0002-2973-5321

Notes

The authors declare no competing financial interest.

■ ACKNOWLEDGMENTS

The authors wish to thank The Netherlands Organization for Scientific Research (NWO/CW) for financial support.

■ REFERENCES

(1) Jeffrey, G. A. *An Introduction to Hydrogen Bonding*; Oxford University Press: New York, 1997.

(2) Moran, L. A.; Horton, H. R.; Scrimgeour, K. G.; Perry, M. D. *Principles of Biochemistry*, 5th ed.; Pearson Education: New York, 2012.

(3) Nelson, D. L.; Cox, M. M. *Lehninger Principles of Biochemistry*, 6th ed.; W. H. Freeman and Company: New York, 2012.

(4) Sijbesma, R. P.; Beijer, F. H.; Brunsveld, L.; Folmer, B. J. B.; Hirschberg, J. H. K Ky; Lange, R. F. M.; Lowe, J. K. L.; Meijer, E. W.

DOI: 10.1021/acs.jpca.7b12635
J. Phys. Chem. A 2018, 122, 1813−1820

Reversible Polymers Formed from Self-Complementary Monomers Using Quadruple Hydrogen Bonding. *Science* **1997**, *278*, 1601−1604.
(5) Kuhn, B.; Mohr, P.; Stahl, M. Intramolecular Hydrogen Bonding in Medicinal Chemistry. *J. Med. Chem.* **2010**, *53*, 2601−2611.
(6) Gale, P. A., Steed, J. W., Eds. *Supramolecular Chemistry: From Molecules to Nanomaterials*; Wiley: Chichester, 2012.
(7) Pellizzaro, M. L.; Houton, K. A.; Wilson, A. J. Sequential and Phototriggered Supramolecular Self-sorting Cascades Using Hydrogen-bonded Motifs. *Chem. Sci.* **2013**, *4*, 1825−1829.
(8) Persch, E.; Dumele, O.; Diederich, F. Molecular Recognition in Chemical and Biological Systems. *Angew. Chem., Int. Ed.* **2015**, *54*, 3290−3327.
(9) Roy, N.; Bruchmann, B.; Lehn, J-M. DYNAMERS: Dynamic Polymers as Self-Healing Materials. *Chem. Soc. Rev.* **2015**, *44*, 3786−3807.
(10) Yang, L.; Tan, X.; Wang, Z. Zhang X. Supramolecular Polymers: Historical Development, Preparation, Characterization, and Functions. *Chem. Rev.* **2015**, *115*, 7196−7239.
(11) Arunan, E.; Desiraju, G. R.; Klein, R. A.; Sadlej, J.; Scheiner, S.; Alkorta, I.; Clary, D. C.; Crabtree, R. H.; Dannenberg, J. J.; Hobza, P.; et al. Defining the Hydrogen Bond: An Account (IUPAC Technical Report). *Pure Appl. Chem.* **2011**, *83*, 1619−1636. and references therein.
(12) Grabowski, S. J. What is the Covalency of Hydrogen Bonding? *Chem. Rev.* **2011**, *111*, 2597−2625. and references therein.
(13) Umeyama, H.; Morokuma, K. The Origin of Hydrogen Bonding. An Energy Decomposition Study. *J. Am. Chem. Soc.* **1977**, *99*, 1316−1332.
(14) Fonseca Guerra, C.; Bickelhaupt, F. M.; Snijders, J. G.; Baerends, E. J. The Nature of the Hydrogen Bond in DNA Base Pairs: The Role of Charge Transfer and Resonance Assistance. *Chem. - Eur. J.* **1999**, *5*, 3581−3594.
(15) Poater, J.; Fradera, X.; Solà, M.; Duran, M.; Simon, S. On the Electron-pair Nature of the Hydrogen Bond in the Framework of the Atoms in Molecules Theory. *Chem. Phys. Lett.* **2003**, *369*, 248−255.
(16) Fonseca Guerra, C.; Zijlstra, H.; Paragi, G.; Bickelhaupt, F. M. Telomere Structure and Stability: Covalency in Hydrogen Bonds, Not Resonance Assistance, Causes Cooperativity in Guanine Quartets. *Chem. - Eur. J.* **2011**, *17*, 12612−12622.
(17) Elgabarty, H.; Khaliullin, R. Z.; Kühne, T. D. Covalency of Hydrogen Bonds in Liquid Water Can Be Probed by Proton Nuclear Magnetic Resonance Experiments. *Nat. Commun.* **2015**, *6*, 8318.
(18) Hujo, W.; Grimme, S. Performance of Non-Local and Atom-Pairwise Dispersion Corrections to DFT for Structural Parameters of Molecules with Noncovalent Interactions. *J. Chem. Theory Comput.* **2013**, *9*, 308−315.
(19) van der Lubbe, S. C. C.; Fonseca Guerra, C. Hydrogen-Bond Strength of CC and GG Pairs Determined by Steric Repulsion: Electrostatics and Charge Transfer Overruled. *Chem. - Eur. J.* **2017**, *23*, 10249−10253.
(20) Gilli, G.; Bellucci, F.; Ferretti, V.; Bertolasi, V. Evidence for Resonance-Assisted Hydrogen Bonding from Crystal-Structure Correlations on the Enol Form of the β-Diketone Fragment. *J. Am. Chem. Soc.* **1989**, *111*, 1023−1028.
(21) Bertolasi, V.; Gilli, P.; Ferretti, V.; Gilli, G. Evidence for Resonance-Assisted Hydrogen Bonding. 2. Intercorrelation between Crystal Structure and Spectroscopic Parameters in Eight Intramolecularly Hydrogen Bonded 1,3-Diaryl-1,3-propanedione Enols. *J. Am. Chem. Soc.* **1991**, *113*, 4917−4925.
(22) Gora, R. W.; Grabowski, S. J.; Leszczynski, J. Dimers of Formic Acid, Acetic Acid, Formamide and Pyrrole-2-carboxylic Acid: An Ab Initio Study. *J. Phys. Chem. A* **2005**, *109*, 6397−6405.
(23) Gora, R. W.; Maj, M.; Grabowski, S. J. Resonance-Assisted Hydrogen Bonding Revisited. Resonance Stabilization *vs.* Charge Delocalization. *Phys. Chem. Chem. Phys.* **2013**, *15*, 2514−2522.
(24) Beck, J. F.; Mo, Y. How Resonance Assists Hydrogen Bonding Interactions: An Energy Decomposition Analysis. *J. Comput. Chem.* **2007**, *28*, 455−466.
(25) Jiang, X.; Zhang, H.; Wu, W.; Mo, Y. A Critical Check for the Role of Resonance in Intramolecular Hydrogen Bonding. *Chem. - Eur. J.* **2017**, *23*, 16885−16891.
(26) Lin, X.; Zhang, H.; Jiang, X.; Wu, W.; Mo, Y. The origin of the Non-Additivity in Resonance-Assisted Hydrogen Bond Systems. *J. Phys. Chem. A* **2017**, *121*, 8535−8541.
(27) Guillaumes, L.; Simon, S.; Fonseca Guerra, C. The Role of Aromaticity, Hybridization, Electrostatics, and Covalency in Resonance-Assisted Hydrogen Bonds of Adenine−Thymine (AT) Base Pairs and Their Mimics. *ChemistryOpen* **2015**, *4*, 318−327.
(28) Alkorta, I.; Elguero, J.; Mó, O.; Yáñez, M.; Del Bene, J. E. Do Coupling Constants and Chemical Shifts Provide Evidence for the Existence of Resonance-Assisted Hydrogen Bonds? *Mol. Phys.* **2004**, *102*, 2563−2574.
(29) Sanz, P.; Mó, O.; Yáñez, M.; Elguero, J. Resonance-Assisted Hydrogen Bonds: A Critical Examination. Structure and Stability of the Enols of β-Diketones and β-Enaminones. *J. Phys. Chem. A* **2007**, *111*, 3585−3591.
(30) Te Velde, G.; Bickelhaupt, F. M.; Baerends, E. J.; Fonseca Guerra, C.; van Gisbergen, S. J. A.; Snijders, J. G.; Ziegler, T. Chemistry with ADF. *J. Comput. Chem.* **2001**, *22*, 931−967.
(31) Becke, A. D. Density-functional Exchange-Energy Approximation with Correct Asymptotic Behavior. *Phys. Rev. A: At., Mol., Opt. Phys.* **1988**, *38*, 3098−3100.
(32) Perdew, J. P. Density-Functional Approximation for the Correlation Energy of the Inhomogeneous Electron Gas. *Phys. Rev. B: Condens. Matter Mater. Phys.* **1986**, *33*, 8822−8824.
(33) Šponer, J.; Jurečka, P.; Hobza, P. Accurate Interaction Energies of Hydrogen-Bonded Nucleic Acid Base Pairs. *J. Am. Chem. Soc.* **2004**, *126*, 10142−10151.
(34) Jurečka, P.; Šponer, J.; Černy, J.; Hobza, P. Benchmark Database of Accurate (MP2 and CCSD(T) Complete Basis Set Limit) Interaction Energies of Small Model Complexes, DNA Base Pairs, and Amino Acid Pairs. *Phys. Chem. Chem. Phys.* **2006**, *8*, 1985−1993.
(35) Fonseca Guerra, C.; van der Wijst, T.; Poater, J.; Swart, M.; Bickelhaupt, F. M. Adenine versus Guanine Quartets in Aqueous Solution: Dispersion-Corrected DFT study on the Differences in π-stacking and Hydrogen-Bonding Behavior. *Theor. Chem. Acc.* **2010**, *125*, 245−252.
(36) Snijders, J. G.; Vernooijs, P.; Baerends, E. J. Roothaan-Hartree-Fock-Slater Atomic Wave Functions. Single-Zeta, Double-Zeta, and Extended Slater-Type Basis Sets for $_{87}$Fr-$_{103}$Lr. *At. Data Nucl. Data Tables* **1981**, *26*, 483−509.
(37) Baerends, E. J.; Ellis, D. E.; Ros, P. Self-Consistent Molecular Hartree-Fock-Slater Calcuations I. The Computational Procedure. *Chem. Phys.* **1973**, *2*, 41−51.
(38) Legault, C. Y. *CYLview 1.0b*; Université de Sherbrooke, Sherbrooke, 2009 (http://www.cylview.org).
(39) Bickelhaupt, F. M.; Baerends, E. J. Kohn-Sham Density Functional Theory: Predicting and Understanding Chemistry. In *Reviews in Computational Chemistry*; Lipkowitz, K. B., Boyd, D. B., Eds.; John Wiley & Sons, Inc.: Hoboken, NJ, 2000; Vol. *15*, pp 1−81.
(40) Fonseca Guerra, C.; Handgraaf, J. − W.; Baerends, E. J.; Bickelhaupt, F. M. Voronoi Deformation Density (VDD) Charges: Assessment of the Mulliken, Bader, Hirshfeld, Weinhold, and VDD Methods for Charge Analysis. *J. Comput. Chem.* **2004**, *25*, 189−210.
(41) Voronoi, G. Recherches sur les Paralléloèdres Primitives. *J. Reine Angew. Math.* **1908**, *134*, 198−287.
(42) Sanz, O.; Mó, O.; Yáñez, M.; Elguero, J. Non-Resonance-Assisted Hydrogen Bonding in Hydroxymethylene and Aminomethylene Cyclobutanones and Cyclobutenones and Their Nitrogen Counterparts. *ChemPhysChem* **2007**, *8*, 1950−1958.
(43) Sanz, O.; Mó, O.; Yáñez, M.; Elguero, J. Bonding in Tropolone, 2-Aminotropone, and Aminotroponimine: No Evidence of Resonance-Assisted Hydrogen-Bond Effects. *Chem. - Eur. J.* **2008**, *14*, 4225−4232.
(44) Jabloński, M.; Kaczmarek, A.; Sadlej, A. J. Estimates of the Energy of Intramolecular Hydrogen Bonds. *J. Phys. Chem. A* **2006**, *110*, 10890−10898.

DOI: 10.1021/acs.jpca.7b12635
J. Phys. Chem. A 2018, 122, 1813−1820

(45) Woodford, J. N. Density Functional Theory and Atoms-in-Molecules Investigation of Intramolecular Hydrogen Bonding in Derivatives of Malonaldehyde and Implications for Resonance-Assisted Hydrogen Bonding. *J. Phys. Chem. A* **2007**, *111*, 8519−8530.
(46) Nekoei, A. R.; Vatanparast, M. An Intramolecular Hydrogen Bond Study in Some Schiff Bases of Fulvene: A Challenge Between the RAHB Concept and the σ-Skeleton Influence. *New J. Chem.* **2014**, *38*, 5886−5891.

DOI: 10.1021/acs.jpca.7b12635
J. Phys. Chem. A 2018, 122, 1813−1820